Pallidal Dysfunction Drives a Cerebellothalamic Circuit into Parkinson Tremor

Rick C. Helmich, MD,[1,2] Marcel J. R. Janssen, MD, PhD,[3] Wim J. G. Oyen, MD, PhD,[3] Bastiaan R. Bloem, MD, PhD,[2] and Ivan Toni, PhD[1]

Objective: Parkinson disease (PD) is characterized by striatal dopamine depletion, which explains clinical symptoms such as bradykinesia and rigidity, but not resting tremor. Instead, resting tremor is associated with increased activity in a distinct cerebellothalamic circuit. To date, it remains unknown how the interplay between basal ganglia and the cerebellothalamic circuit can result in resting tremor.
Methods: We studied 21 tremor-dominant PD patients, 23 nontremor PD patients, and 36 controls. Using functional magnetic resonance imaging, we measured functional connectivity between basal ganglia nuclei (globus pallidus internus [GPi], globus pallidus externus [GPe], putamen, caudate) and the cerebellothalamic circuit. Using electromyography during scanning, we measured tremor-related activity in the basal ganglia and cerebellothalamic circuit. We also quantified striatopallidal dopamine depletion using iodine-123-N-omega-fluoropropyl-2β-carbomethoxy-3β-(4-iodophenyl)tropane [[I-123]FP-CIT] single photon emission computed tomography.
Results: Pallidal (but not striatal) dopamine depletion correlated with clinical tremor severity. The GPi, GPe, and putamen were transiently activated at the onset of tremor episodes, whereas activity in the cerebellothalamic circuit cofluctuated with tremor amplitude. The GPi and putamen of tremor-dominant PD patients had increased functional connectivity with the cerebellothalamic circuit, which was relegated through the motor cortex.
Interpretation: Resting tremor may result from a pathological interaction between the basal ganglia and the cerebellothalamic circuit. The cerebellothalamic circuit, which controls tremor amplitude, appears to be driven into tremor generation when receiving transient signals from the dopamine-depleted basal ganglia. This may explain why basal ganglia dysfunction is required for developing resting tremor, although a cerebellothalamic circuit produces it. Our model also clarifies why neurosurgical interventions targeted at either the basal ganglia or the cerebellothalamic circuit can both suppress tremor.

ANN NEUROL 2011;69:269–281

The primary pathophysiological substrate of Parkinson disease (PD) involves dopamine depletion in the striatum.[1] This disrupts corticostriatal processing and explains clinical symptoms such as rigidity and bradykinesia, but not resting tremor.[2] Conversely, resting tremor is associated with a distinct cerebellothalamic circuit[3,4] involving the ventral intermediate nucleus of the thalamus (VIM), motor cortex (MC), and cerebellum (CBLM). This VIM–MC–CBLM circuit is shared with other tremor types such as physiological tremor[5] and essential tremor,[6] suggesting a fundamental role in generating rhythmic oscillatory motor ouput.[7] However, to date it remains unknown how basal ganglia dysfunction in PD can drive the distinct VIM–MC–CBLM circuit into generating resting tremor.[8] Tremor-related responses have been observed both in the basal ganglia (pallidum,[9,10] subthalamic nucleus[11]) and in the cerebellothalamic circuit (VIM[12]), and interference with either circuit can effectively suppress resting tremor.[13–15] This suggests that resting tremor results from a pathological interaction between the basal ganglia and the VIM–MC–CBLM circuit.[16] It has been suggested that this

View this article online at wileyonlinelibrary.com. DOI: 10.1002/ana.22361

Received Jul 30, 2010, and in revised form Dec 15, 2010. Accepted for publication Dec 17, 2010.

Address correspondence to Dr Helmich, MD, Donders Centre for Brain, Cognition, and Behavior, Center for Neuroscience, Department of Neurology (HP 935), PO Box 9101, 6500 HB Nijmegen, the Netherlands. E-mail: R.Helmich@neuro.umcn.nl

From the [1]Donders Institute for Brain, Cognition, and Behavior, Center for Cognitive Neuroimaging, Radboud University Nijmegen; [2]Department of Neurology and Parkinson Center Nijmegen, Radboud University Nijmegen Medical Center; and [3]Department of Nuclear Medicine, Radboud University Nijmegen Medical Center, Nijmegen, the Netherlands.

Additional supporting information can be found in the online version of this article.

interaction occurs in MC,[16] given the dense anatomical connectivity of the basal ganglia with the MC,[17] but not with the VIM[18] and only sparsely with the CBLM.[19] Thus, pathological signals from the basal ganglia may be transmitted to the VIM–MC–CBLM circuit via the MC, driving this physiological network into resting tremor. Accordingly, coherence between VIM neurons and resting tremor is strong and consistent,[12] whereas coherence between pallidal neurons and resting tremor is transient and intermittent.[9,10] This suggests that the basal ganglia have a modulatory role in tremor genesis, whereas the VIM–MC–CBLM circuit drives the tremor on a cycle-by-cycle basis.[3,4] The role of the pallidum in resting tremor is further supported by postmortem work; pallidal (but not striatal) dopamine depletion predicts tremor severity,[20] possibly caused by degeneration of specific portions of the midbrain.[21]

We hypothesize that altered interactions between the dopamine-depleted basal ganglia and the VIM–MC–CBLM circuit mediate the occurrence of resting tremor in PD. We test this hypothesis by exploiting a well-established clinical distinction between 2 PD subtypes that are characterized by the presence or absence of tremor, whereas bradykinesia and rigidity are expressed in both groups.[22] Using functional magnetic resonance imaging (fMRI) and concurrent electromyographic (EMG) recordings, we quantified functional connectivity between the basal ganglia and the VIM–MC–CBLM circuit, and the relation between ongoing cerebral activity (as indexed by intrinsic fluctuations in the blood oxygenation level dependent [BOLD] signal) and spontaneous changes in tremor amplitude. Using iodine-123-N-omega-fluoropropyl-2β-carbomethoxy-3β-(4-iodophenyl)tropane [[I-123]FP-CIT] single photon emission computed tomography (SPECT), we compared striatopallidal dopamine transporter concentrations between tremor-dominant and nontremor PD patients.

Subjects and Methods

Subjects

Three groups of 36 controls (18 men; aged 57 $\pm$ 1 years, average $\pm$ standard error of the mean [SEM]), 21 tremor-dominant PD patients (12 men; 58 $\pm$ 2 years), and 23 nontremor PD patients (18 men; 58 $\pm$ 2 years) were measured. Age and gender did not significantly differ between groups ($p > 0.05$). All subjects were right-handed and gave written informed consent before participation. Patients were included when they had idiopathic PD, diagnosed according to the UK Brain Bank criteria. Exclusion criteria were: cognitive dysfunction (ie, Mini-Mental State Examination <24), neurological comorbidity, moderate to severe head tremor, dyskinesias, and general exclusion criteria for MRI scanning. Tremor-dominant PD was defined as a Unified Parkinson Disease Rating Scale (UPDRS) resting tremor score of $\geq$2 for at least 1 hand during physical examination, and a history of resting tremor. Nontremor PD was defined as a UPDRS resting tremor score of 0 during physical examination and no history of resting tremor. Both PD groups were carefully matched for general disease severity, cognitive function, and severity of bradykinesia and rigidity, but differed on resting tremor scores (Table 1). Twelve patients used no Parkinson medication; the others used dopaminergic medication (L-dopa or dopamine agonists). The amount of dopaminergic medication was similar between groups ($p > 0.1$; see Supplementary Material), and was added as a covariate to all group analyses. All patients were measured off medication, that is, at least 12 hours after the last dose.[23]

Image Acquisition and Preprocessing

MRI was performed in 19 tremor-dominant patients, 23 nontremor patients, and 36 healthy controls, on a 3T MRI system (Siemens, Erlangen, Germany). Subjects were instructed to lie still with eyes closed, and to avoid falling asleep (confirmed with a postscan debriefing). Functional data were collected using a single-shot gradient echo-planar imaging sequence (echo time [TE]/repetition time [TR] = 30/1,450 milliseconds; 21 axial slices; voxel size = 3.5 $\times$ 3.5 $\times$ 5.0 mm; interslice gap = 1.5 mm; field of view [FOV] = 224 mm; scanning time = $\sim$6 minutes; 265 images). Anatomical data were acquired using an magnetization prepared-rapid gradient echo sequence (TE/TR = 2.92/2,300 milliseconds; voxel size = 1.0 $\times$ 1.0 $\times$ 1.0 mm; 192 sagittal slices; FOV = 256 mm). Data were preprocessed and analyzed with SPM5 (www.fil.ion.ucl.ac.uk/spm; see Supplementary Material). Images used in the functional connectivity analyses were low-pass filtered to retain frequencies <0.1 Hz. Head movements during scanning did not differ between tremor-dominant and nontremor PD patients (see Supplementary Material).

Regions of Interest

We focused our analyses on the VIM–MC–CBLM circuit and the basal ganglia (globus pallidus internus [GPi], globus pallidus externus [GPe], putamen, caudate). The VIM–MC–CBLM circuit was localized on the basis of a whole-brain search for tremor-related cerebral activity (see below). The basal ganglia circuit was identified on the basis of anatomical criteria (see Supplementary Material). We averaged cerebral effects (beta values) across all voxels of each region and performed statistical analyses on these values in SPSS.15 (SPSS Inc., Chicago, IL).

Tremor-Related Activity

Using EMG, we measured muscle activity in the most-affected arm of 19 tremor-dominant PD patients, 23 nontremor PD patients, and 23 controls during magnetic resonance scanning (see Supplementary Material and Helmich et al[24]). For each tremor-dominant patient, we calculated scan-by-scan EMG power at the patient's tremor frequency (average = 4.4 $\pm$ 0.2Hz; Supplementary Fig 1), resulting in patient-specific

TABLE 1: Clinical Characteristics

Group	Tremor-dominant PD (n = 21)	Nontremor PD (n = 23)	*p*
Duration	4.9 (2.6)	4.8 (2.7)	0.92
H & Y	2.1 (0.3)	2.1 (0.2)	0.82
FAB	16.8 (1.0)	17.1 (1.1)	0.32
UPDRS			
Total	28.4 (8.6)	28.0 (8.4)	0.87
Nontremor (B + R)			
Most	10.5 (2.6)[a]	11.0 (3.0)[a]	0.61
Least	4.7 (3.7)	6.0 (3.5)	0.21
Axial	7.3 (3.6)	9.2 (4.0)	0.11
TRS			
Rest			
Most	3.4 (1.4)[a]	0.2 (0.5)	<0.001[b]
Least	0.6 (1.0)	0.0 (0.0)	0.01[b]
Posture			
Most	1.9 (1.1)[a]	1.0 (1.4)	0.04[b]
Least	0.5 (0.9)	0.4 (0.8)	0.7
Action			
Most	0.7 (0.9)	0.7 (0.9)	0.81
Least	0.4 (0.6)	0.3 (0.6)	0.46

Disease characteristics of tremor-dominant and non-tremor Parkinson disease (PD) patients are shown (average, standard deviation in parentheses) and compared between groups
(2-sample *t* tests, 2-tailed). Each patient's disease severity was assessed using the Hoehn & Yahr (H & Y maximum is 5) stages and the Unified Parkinson Disease Rating Scale part III (UPDRS; maximum score is 108). B + R = limb bradykinesia and rigidity (sum of UPDRS items 22–26). Axial = axial symptoms (sum of UPDRS items 18, 19, 22, and 27–31). Cognitive function was assessed with the Frontal Assessment Battery (FAB[37]; maximum is 18). Duration was defined as the time since subjective symptom onset (in years). In most patients (18 tremor-dominant, 20 nontremor), tremor severity was assessed using Part A of the Fahn–Tolosa–Marin Tremor Rating Scale (TRS; maximum is 8 points for each side). The TRS involves a clinical score of 0–4 points for each extremity (hands/feet, left/right), separately for resting, postural, and action tremor.[38] Three nontremor patients had a very subtle resting tremor while off medication on the day of testing, explaining the nonzero resting tremor score. All patients had asymmetric symptoms (), but the most-affected side (left/right) did not differ between groups ($p = 0.24$, chi-square test).
[a]$p < 0.001$ on a paired-samples *t* test comparing the most-affected compared to least-affected side for each group.
[b]Statistically significant.

regressors describing fluctuations in tremor amplitude (EMG AMP). To capture changes in tremor amplitude (EMG on/offset), we calculated the temporal derivative of the EMG AMP regressor. After convolution of both regressors with a hemodynamic response function, we considered EMG AMP and EMG on/offset as explanatory variables in a multiple regression analysis. We also included a set of nuisance regressors, as described in the Supplementary Material. Parameter estimates (beta values) for all regressors were obtained by maximum likelihood estimation, modeling temporal autocorrelation as an AR(1) process. The effect of each EMG regressor was tested at the group level using 1-sample *t* tests (1-tailed). The effects of each EMG regressor were compared between the most-affected and least-affected hemispheres using paired-sample *t* tests (1-tailed). We assessed the correlation between tremor-related responses and clinical resting tremor severity by using within-patient difference scores (between most-affected and least-affected sides), thereby controlling for nonspecific differences between patients.

Functional Connectivity between the Basal Ganglia and VIM–MC–CBLM Circuit

We performed separate seed-based functional connectivity analyses for the left and right GPi, GPe, putamen, and caudate. MarsBaR (http://marsbar.sourceforge.net) was used to extract the average time courses from these regions. For each subject and each region, we then entered this regressor in a multiple

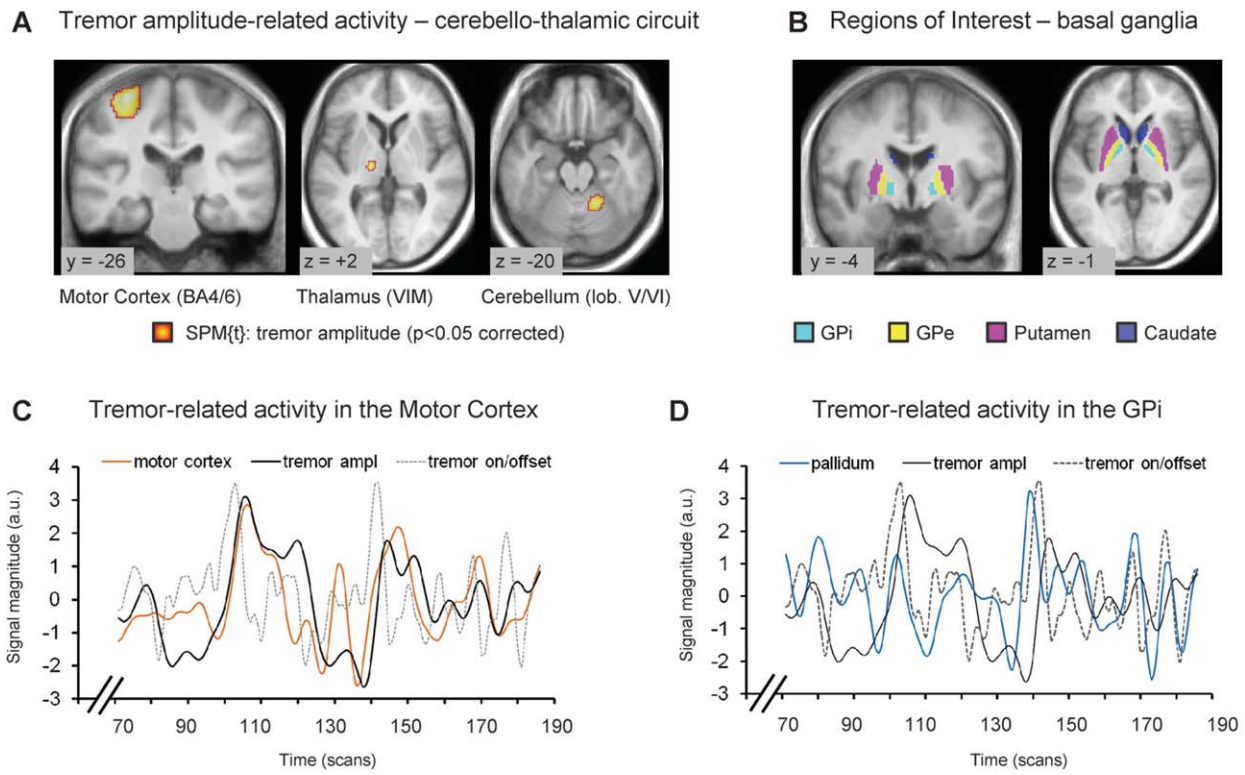
A Tremor amplitude-related activity – cerebello-thalamic circuit
y = -26
z = +2
z = -20
Motor Cortex (BA4/6)
Thalamus (VIM)
Cerebellum (lob. V/VI)
SPM{t}: tremor amplitude (p<0.05 corrected)
B Regions of Interest – basal ganglia
y = -4
z = -1
GPi
GPe
Putamen
Caudate
C Tremor-related activity in the Motor Cortex
motor cortex
tremor ampl
tremor on/offset
Signal magnitude (a.u.)
Time (scans)
D Tremor-related activity in the GPi
pallidum
tremor ampl
tremor on/offset
Signal magnitude (a.u.)
Time (scans)
Tremor-related activity in the cerebello-thalamic circuit
E Thalamus (VIM)
F Cerebellum (lob. V/VI)
G Motor Cortex (BA4/6)
H Motor Cortex
most-affected
least-affected
Cerebral activity (beta)
tremor amplitude
tremor on/offset
R² = .52; p = .001
Tremor score (Δ-TRS)
Activity (tremor amp; Δ-β weight)
Tremor-related activity in the basal ganglia
I GPi
J GPe
K Putamen
L Caudate nucleus

FIGURE 1

regression analysis together with several nuisance regressors (see Supplementary Material). To isolate altered functional connectivity over and above tremor-related effects, we added the EMG AMP and EMG on/offset regressors to the first-level models of tremor-dominant patients. For each basal ganglia region (GPi, GPe, putamen, and caudate) we performed 2 group analyses. First, we used the asymmetric nature of PD to compare functional connectivity of the most-affected and least-affected basal ganglia nucleus with the VIM, MC, and CBLM in the corresponding hemisphere. Specifically, we performed a 2-way analysis of variance (ANOVA) with factors Group (19 tremor-dominant, 23 nontremor) and Hemisphere (most affected, least affected) for MC, VIM, and CBLM. Second, we directly compared basal ganglia connectivity between tremor-dominant PD and healthy controls, in the same way as described above. Because there were significant differences between the most-affected and least-affected hemispheres in the tremor-dominant group, and because the most-affected side was not the same across all PD patients, we compared left hemisphere-affected PD patients (13 tremor-dominant) with 36 controls. Finally, we related altered connectivity to clinical symptoms, that is, we correlated the difference between functional connectivity (for example, GPi–MC) of the most-affected and least-affected side with the difference between clinical disease severity scores of the most-affected and least-affected side (Pearson correlation, 1-tailed). This was done both for resting tremor (using the Tremor Rating Scale [TRS]) and for bradykinesia (using UPDRS items 23–26) in the 16 tremor-dominant patients where we obtained TRS scores.

Imaging of the Dopamine Transporter

Thirty-five PD patients (16 tremor-dominant, 19 nontremor) received a [I-123]FP-CIT SPECT scan on a separate day within 3 months after the fMRI scan. After image preprocessing (Supplementary Material), we calculated the average amount of dopamine transporter (DAT) binding in the left and right pallidum, putamen, and caudate (with the bilateral occipital cortex as reference region). Because we did not want to claim more spatial resolution than SPECT can offer, and because tremor-related activity and connectivity were similar for GPi and GPe, we averaged DAT binding across these 2 regions. Using ANOVA, we compared DAT binding between factors Region (putamen, caudate, and pallidum), Group (tremor-dominant, nontremor) and Side (most affected, least affected). We also related DAT binding to clinical symptoms (resting tremor and bradykinesia, see above). Thus, for each region we correlated the difference between DAT binding of the most-affected and least-affected side with the difference between clinical disease severity scores of the most-affected and least-affected side (Pearson correlation, 1-tailed).

Results

Tremor-Related Activity in PD

Using combined EMG-fMRI, we isolated 2 distinct patterns of tremor-related activity. This approach is illustrated in Figure 1C–D for 1 patient. Group effects are shown in Figure 1; statistics are listed in Tables 2 and 3. First, fluctuations in tremor amplitude (EMG AMP) accounted for a significant portion of cerebral activity in the contralateral MC, contralateral VIM, and ipsilateral CBLM ($p < 0.05$, whole-brain corrected; see Table 2). In all 3 regions, tremor-related activity was stronger in the most-affected than in the least-affected hemisphere. Furthermore, tremor-related activity increased with clinical tremor scores in the MC and CBLM (see Table 3). Conversely, there were no tremor amplitude-related effects in the basal ganglia. Second, changes in tremor amplitude (EMG on/offset) evoked additional cerebral effects in the most-affected MC/CBLM, bilateral VIM, and in the basal ganglia (GPi, GPe, and putamen). Crucially, these effects were not observed in cognitive portions of the striatum (ie, the caudate). In the MC, CBLM, and in the putamen, these effects were stronger in the most-affected than in the least-affected hemisphere. Furthermore, cerebral responses in the MC increased with clinical tremor scores.

◀ **FIGURE 1: Tremor-related cerebral activity in tremor-dominant Parkinson disease (PD). (A) Cerebral regions where activity cofluctuated with tremor amplitude (Statistical Parametric Mapping [SPM] t-contrast on the electromyographic (EMG) amplitude regressor in 19 tremor-dominant patients, shown at a threshold of $p < 0.05$ cluster-level corrected for multiple comparisons, using an intensity threshold of $T > 3.6$). Activity was localized to the motor cortex (MC), ventral intermediate nucleus of the thalamus (VIM), and cerebellum. The left side is the side contralateral to the tremor. In these regions of the cerebellothalamic circuit, and in the 4 basal ganglia nuclei shown in panel B, we quantified 2 separate effects: (1) cerebral activity related to tremor amplitude; (2) cerebral activity related to changes in tremor amplitude (tremor on/offset). Panels C and D illustrate this for 1 patient. Three relevant time courses are shown: (1) brain activity (MC in orange in panel C, globus pallidus internus [GPi] in blue in panel D, both z-normalized); (2) tremor amplitude of the contralateral hand (in black; EMG regressor convolved with the hrf; z-normalized); (3) tremor on/offset (in dotted gray, first temporal derivative of the tremor amplitude regressor, convolved with the hrf; z-normalized). Whereas MC activity clearly correlated with tremor amplitude (C), this pattern was not observed for the GPi (D). Conversely, GPi activity correlated with changes in tremor amplitude (the on/offset regressor, which peaks when the tremor changes from low to high amplitude). Panels E–L show these effects for the whole group (n = 19 tremor-dominant PD patients), separately for the most-affected (*red bars*) and for the least-affected (*green bars*) hemisphere. Panel H shows the relationship between tremor-related activity in the MC (on the x-axis) and clinical tremor severity (on the y-axis). Both effects are quantified as the difference (Δ) between parameters relative to the most-affected and least-affected side. a.u. = arbitrary units; BA = Brodmann area; hrf = haemodynamic response function; lob. = lobule; GPe = globus pallidus externus; TRS = Tremor Rating Scale; see Tables 2 and 3 for statistics.**

TABLE 2: Region Showing Tremor Amplitude-Related Brain Activity

Anatomical Label	Anatomical Location	Hemisphere (wrt Tremor)	T	*p* (corrected)	Cluster Size (voxels)	Stereotactic Coordinates (x y z) in MNI Space		
MC	BA4 (60% overlap); BA6 (26% overlap)	Contralateral	6.1	<0.001	464	±28	−26	+62
CBLM	Lobule V (39% overlap); lobule VI (49% overlap)	Ipsilateral	5.5	0.004	177	±18	−50	−20
VIM	Within thalamotomy region (VIM)[39]	Contralateral	4.8	0.030	121	±12	−18	+2

Spatial coordinates of the local maxima of regions where activity cofluctuated with tremor amplitude in 19 tremor-dominant Parkinson disease patients. All results are corrected for multiple comparisons across the whole brain ($p < 0.05$ FWE-corrected at the cluster level, using an intensity threshold of $T > 3.6$). The motor cortex (MC) and cerebellum (CBLM) clusters were localized using cytoarchitectonic probability maps (Anatomy Toolbox[40]). The thalamic cluster was localized using stereotactic coordinates of deep brain surgery (ventral intermediate nucleus of the thalamus [VIM] thalamotomy for treatment of parkinsonian tremor[39]). The first 2 local maxima were located <5 mm from the optimal site for thalamotomy.[39] This location, at the border of the cerebellar thalamus (ventral lateral posterior nucleus [VLp] according Jones[42]; VIM according to Hassler[43]) and the somatosensory thalamus (ventral posterior lateral nucleus pars posterior [VPLp] according to Jones[42]) was confirmed by a stereotactic atlas of the human thalamus[41] (see Supplementary Material for details).
MNI = Montreal Neurological Institute.

Increased Interactions between Basal Ganglia and VIM–MC–CBLM Circuit in Tremor-Dominant PD

We tested the hypothesis that increased functional interactions between the basal ganglia (GPi, GPe, putamen, and caudate) and the VIM–MC–CBLM circuit mediate the occurrence of resting tremor in PD. Group effects are shown in Figure 2; statistics are listed in Table 4. First, tremor-dominant PD patients had enhanced GPi–MC and putamen–MC coupling compared to nontremor PD patients, and these effects were specific for the most-affected hemisphere (Group × Side interaction; see Table 4 and Fig 2). In contrast, there were no significant group differences for GPe–MC and caudate–MC coupling. Second, we directly compared healthy controls with left hemisphere-affected tremor-dominant patients. This analysis confirmed differential GPi–MC and putamen–MC coupling between groups and hemispheres (Group × Side interaction). Specifically, tremor-dominant patients had larger GPi–MC and putamen–MC coupling in the left (ie, most affected) hemisphere than controls ($p < 0.001$). Conversely, both groups had similar coupling in the right (ie, least affected) hemisphere ($p > 0.05$). These effects were not significant for the caudate; there was a nonsignificant trend toward differential GPe–MC coupling between groups and hemispheres. Third, tremor-dominant patients with higher striatopallidal coupling (between GPi/GPe/putamen and MC) showed higher clinical resting tremor scores ($p < 0.05$). These effects were specific for tremor; there were no correlations between striatopallidal coupling and bradykinesia scores ($p > 0.30$). Finally, the increased striatopallidal coupling in the most-affected hemisphere of tremor-dominant PD was specific for the MC; there were no group differences for striatopallidal connectivity with the VIM or CBLM. Together, these results point to a specific functional pathway through which the motor loop of the basal ganglia could trigger tremor-related responses in the VIM–MC–CBLM circuit through the MC.

Imaging of the DAT

We tested whether dopaminergic changes in the basal ganglia were related to resting tremor. A direct comparison of DAT binding between regions (pallidum, putamen, and caudate), sides (most-affected vs least-affected hemisphere), and subtypes (tremor-dominant vs nontremor PD) revealed a significant 3-way interaction ($F_{2,64} = 3.6$; $p = 0.033$). In the pallidum, DAT binding was lower in the most-affected compared to least-affected hemisphere of tremor-dominant compared to nontremor PD (Side × Group interaction; $F_{1,33} = 14.2$; $p = 0.001$). Specifically, compared to nontremor PD, tremor-dominant patients had lower pallidal DAT binding in the most-affected hemisphere ($t[32] = 1.9$; $p = 0.035$, 1-tailed) and higher pallidal DAT binding in the least-affected hemisphere ($t[32] = -2.7$; $p = 0.006$; 1-tailed). Conversely, there was no Group × Side interaction for DAT binding in the putamen or caudate ($p > 0.05$).

TABLE 3: Tremor-Related Responses

	Most-Affected Side		Least-Affected Side		Most- > Least-Affected Side		Correlation with Tremor Severity	
Brain Region	**T**	***p***	**T**	***p***	**T**	***p***	***R***	***p***
EMG amplitude								
MC	See Table 2		0.34	0.37	4.0	<0.001[a]	0.72	0.001[a]
CBLM			0.81	0.21	3.5	0.001[a]	0.60	0.008[a]
VIM			3.02	0.004[a]	2.7	0.008[a]	−0.007	0.49
GPi	−0.48	0.32	−0.56	0.29	0.34	0.37	−0.23	0.19
GPe	0.93	0.18	1.19	0.12	−0.23	0.41	−0.18	0.25
Putamen	1.42	0.087	0.62	0.27	1.95	0.033[a]	−0.39	0.066
Caudate	0.48	0.32	0.76	0.23	−0.63	0.27	0.22	0.21
EMG on/offset								
MC	2.36	0.015[a]	0.13	0.45	1.86	0.040[a]	0.63	0.005[a]
CBLM	1.93	0.035[a]	−0.61	0.28	2.73	0.007[a]	0.14	0.30
VIM	2.59	0.009[a]	2.53	0.010[a]	0.36	0.36	0.16	0.28
GPi	2.13	0.024[a]	1.67	0.056	0.77	0.23	0.014	0.48
GPe	2.37	0.015[a]	1.84	0.041[a]	1.27	0.11	0.33	0.10
Putamen	1.82	0.043[a]	0.80	0.22	2.17	0.022[a]	0.24	0.18
Caudate	0.52	0.31	0.20	0.43	0.50	0.31	−0.11	0.34

This table shows the inferential statistics of tremor-related cerebral activity in 19 tremor-dominant Parkinson disease patients. We tested for cerebral activity that correlated with tremor amplitude (electromyographic [EMG] amplitude regressor), and with changes in tremor amplitude tremor on/offset (EMG on/offset regressor). These effects were quantified for the cerebellothalamic circuit (motor cortex [MC], cerebellum [CBLM], and ventral intermediate nucleus of the thalamus [VIM], regions of interest derived from Table 2) and for the basal ganglia (globus pallidus internus [GPi], globus pallidus externus [GPe], putamen, and caudate, regions of interest anatomically defined). Statistics (1-sample *t* tests across the group) are shown separately for the most-affected and for the least-affected hemisphere, and for direct comparisons between both hemispheres. Our primary hypothesis was that the cerebellothalamic circuit and the motor circuit of the basal ganglia should have distinct tremor-related responses (both within the most-affected hemisphere). To test this hypothesis, we averaged tremor-related activity across the whole VIM–MC–CBLM circuit and across the whole striatopallidal motor circuit (GPi, GPe, and putamen), using Bonferroni-corrected inferences ($p < 0.025$) on 1-sample *t* tests across the group. In the VIM–MC–CBLM circuit, there was significant tremor amplitude-related activity ($t[18] = 6.1$; $p < 0.001$) and tremor on/offset-related activity ($t[18] = 3.3$; $p = 0.002$). Conversely, in the basal ganglia there was no amplitude-related activity ($t[18] = 0.82$; $p = 0.21$), but significant tremor on/offset-related activity ($t[18] = 2.4$; $p = 0.013$). The 2 columns on the right show the Pearson correlation *R* and *p* value (1-tailed) between the cerebral effects (tremor-related activity) and clinical effects (total resting tremor score on the Tremor Rating Scale), both quantified as the difference between the most-affected and least-affected sides.
[a]Significant effects.

Instead, DAT binding in the putamen and caudate was generally lower in the most-affected compared to least-affected hemisphere of both PD groups (main effect of Side; putamen: $F_{1,32} = 48.1$; $p < 0.001$; caudate: $F_{1,32} = 28.2$; $p < 0.001$). Furthermore, there was a trend toward overall lower DAT binding in nontremor compared to tremor-dominant PD (main effect of Group; putamen: $F_{1,32} = 3.3$; $p = 0.080$; caudate: $F_{1,32} = 3.6$; $p = 0.066$). Because pallidal DAT binding was differently modulated by PD group and hemisphere than striatal DAT binding, it is unlikely that the pallidal effects were caused by spillover of signal from the putamen. To directly test this possibility, we compared DAT binding in the most-affected pallidum compared to the most-affected putamen, as a function of PD group. This revealed a significant Group × Region interaction ($F_{1,32} = 8.2$; $p = 0.007$), which was driven by group differences in the most-affected pallidum ($p = 0.035$; see above), but not in the most-affected putamen ($p > 0.1$). Furthermore, DAT binding in the striatum and in the pallidum

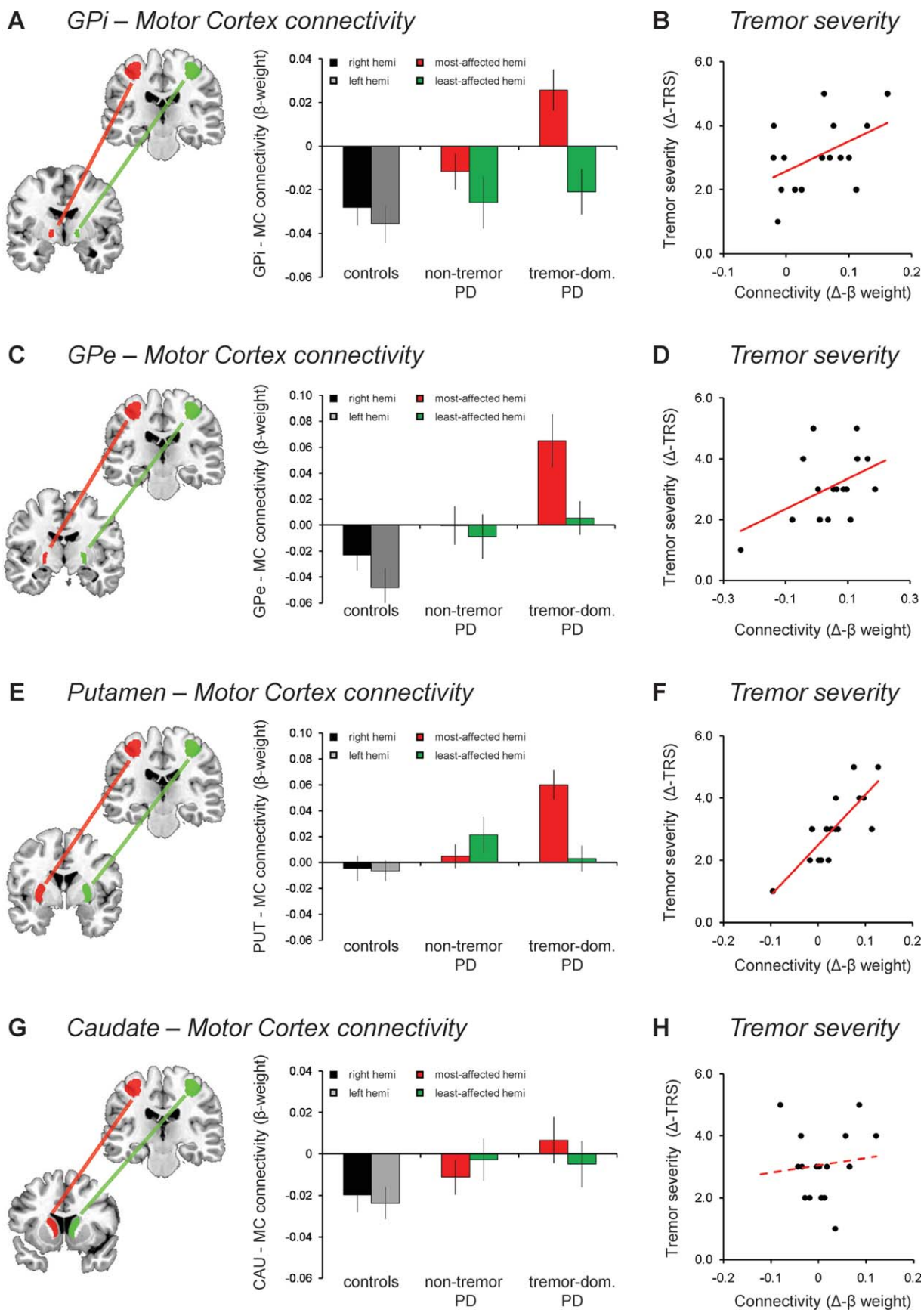
A
GPi – Motor Cortex connectivity
right hemi
left hemi
most-affected hemi
least-affected hemi
GPi - MC connectivity (β-weight)
0.04
0.02
0
-0.02
-0.04
-0.06
controls
non-tremor PD
tremor-dom. PD
B
Tremor severity
Tremor severity (Δ-TRS)
6.0
4.0
2.0
0.0
-0.1
0
0.1
0.2
Connectivity (Δ-β weight)
C
GPe – Motor Cortex connectivity
GPe - MC connectivity (β-weight)
0.10
0.08
0.06
0.04
0.02
0.00
-0.02
-0.04
-0.06
D
Tremor severity
-0.3
-0.1
0.1
0.3
E
Putamen – Motor Cortex connectivity
PUT - MC connectivity (β-weight)
F
Tremor severity
-0.2
-0.1
0
0.1
0.2
G
Caudate – Motor Cortex connectivity
CAU - MC connectivity (β-weight)
H
Tremor severity

FIGURE 2

were correlated with different clinical symptoms. Specifically, bradykinesia correlated with DAT binding in the putamen ($R = 0.52$; $p < 0.001$; Fig 3D) and caudate ($R = 0.50$; $p = 0.001$; Supplementary Fig 4), but not with pallidal DAT binding ($p > 0.05$). Conversely, resting tremor severity correlated with DAT binding in the pallidum ($R = 0.57$; $p = 0.023$; see Fig 3H), but not with DAT binding in the striatum ($p > 0.05$). This correlation remained significant when correcting for DAT binding in putamen and caudate ($R = 0.56$; $p = 0.019$; partial correlation). These findings suggest a specific relationship between pallidal dopamine depletion and resting tremor; tremor-dominant patients had relatively low DAT binding in the most-affected pallidum (compared to their least-affected pallidum and their striatum), and pallidal DAT binding explained individual differences in resting tremor severity.

Discussion

We tested the hypothesis that resting tremor in PD emerges when dopamine depletion in the output layer of the basal ganglia circuitry alters striatopallidal influences on a core cerebellothalamic circuit. There are 4 novel findings. First, activity in the VIM–MC–CBLM circuit cofluctuated with tremor amplitude in PD patients. Second, the most-affected GPi and putamen of tremor-dominant PD patients showed increased functional connectivity with the MC node of the VIM–MC–CBLM circuit. Third, activity in the GPi, GPe, and putamen correlated with onset and offset of tremor episodes, but not with tremor amplitude. Fourth, dopamine depletion in the pallidum, but not the striatum, correlated with tremor severity. These findings suggest that increased interactions between the dopamine-depleted striatopallidal motor loop and the MC provide a neurophysiological context in which transient pallidal fluctuations trigger pathological activity in a VIM–MC–CBLM circuit, leading to the expression of resting tremor in PD (Fig 4).

Parkinson Tremor Emerges from a Physiological VIM–MC–CBLM Circuit

The VIM–MC–CBLM circuit showed tremor-related responses in PD. This finding fits with previous research in PD patients,[3,4,24] and with the dense anatomical connectivity between these 3 areas (as observed in the macaque[17,25,26]). More specifically, it has been suggested that the MC drives the limb tremor,[4] with the CBLM being involved in processing tremor-related afferents[16] and the VIM contributing to both.[12] In healthy subjects, oscillations in the VIM–MC–CBLM circuit have been related to physiological tremor, which occurs during motor execution[5] and may result from central fractionation of motor commands into periodic series of muscle twitches.[27] Accordingly, intrinsic BOLD fluctuations in this same circuit were also strongly coupled in the absence of tremor (in healthy subjects; Supplementary Fig. 3). This supports the notion that correlated activity in the VIM–MC–CBLM circuit is not intrinsically pathological, but already present in the physiological state.

The Striatopallidal Motor Loop Triggers Tremor-Related Activity in the VIM–MC–CBLM Circuit

Tremor-dominant PD patients showed increased functional coupling between the GPi/putamen and the MC node of the VIM–MC–CBLM circuit, as compared to matched nontremor PD patients and healthy controls. This effect was functionally specific in 3 different aspects. First, the increased coupling emerged from the limb-related motor loop of the basal ganglia (GPi, putamen), and it did not extend to the caudate. Second, the magnitude of the coupling predicted the clinical severity of resting tremor, but not bradykinesia. Third, the increased coupling was specific for the most-affected hemisphere. This asymmetry rules out several unspecific sources of altered connectivity, for example, effects caused by differences in patients' arousal, head movements, autonomic fluctuations, vascular changes, or medication status. The tremor-related changes in functional coupling between the basal ganglia and MC were accompanied by specific dopaminergic alterations in the basal ganglia; pallidal dopamine depletion predicted the clinical severity of resting tremor, but not bradykinesia, whereas the opposite pattern was observed for the striatum. This indicates that pallidal (but not striatal) dopamine depletion plays a critical role in the emergence of increased functional

◀ **FIGURE 2: Altered coupling between basal ganglia and motor cortex in tremor-dominant Parkinson's disease (tremor-dom. PD). (A, C, E, G) Functional coupling between a basal ganglia seed region (globus pallidus internus [GPi], globus pallidus externus [GPe], putamen, or caudate [CAU]) and the portion of motor cortex (MC) showing tremor-related activity (on the y-axis, mean β-value ± standard error of the mean). These effects are shown separately for the most/least affected hemisphere (hemi) (in PD), or the left/right hemisphere (in controls). (B, D, F, H) Correlations between striatopallidal connectivity with the MC (on the x-axis, difference between most-affected and least-affected sides, Δ-β weight) and resting tremor severity (on the y-axis, difference between most-affected and least-affected sides, Δ-TRS). These results show increased functional coupling between GPi–MC (A) and putamen–MC (E) in the most-affected hemisphere of tremor-dominant PD. A similar (nonsignificant) trend was seen for GPe–MC coupling (C), but there were no group differences for caudate–MC coupling (G). TRS = Tremor Rating Scale; see Table 4 for statistics.**

TABLE 4: Differential Coupling between Striatopallidal Seed Regions and Motor Cortex

	Tremor-Dominant PD (n = 19) vs Nontremor PD (n = 23)			Tremor-Dominant PD (left-affected, n = 13) vs Controls (n = 36)		
Seed Region	**Group × Side**	**Most-Affected Hemisphere**	**Least-Affected Hemisphere**	**Group × Side**	**Left Hemisphere**	**Right Hemisphere**
GPi	$F_{1,39} = 5.6$; $p = 0.020$[a]	$t(41) = 2.3$; $p = 0.024$[a]	$t(41) = -0.33$; $p = 0.74$	$F_{1,47} = 4.3$; $p = 0.044$[a]	$t(47) = 4.0$; $p < 0.001$[a]	$t(47) = 1.5$; $p = 0.14$
GPe	$F_{1,39} = 1.9$; $p = 0.18$	$t(41) = 5.3$; $p = 0.027$[a]	$t(41) = -0.60$; $p = 0.44$	$F_{1,47} = 3.1$; $p = 0.085$	$t(47) = 3.9$; $p < 0.001$[a]	$t(47) = 1.9$; $p = 0.059$
Putamen	$F_{1,39} = 4.5$; $p = 0.040$[a]	$t(41) = 3.5$; $p = 0.001$[a]	$t(41) = 1.2$; $p = 0.27$	$F_{1,47} = 10.5$; $p = 0.002$[a]	$t(47) = 3.6$; $p = 0.001$[a]	$t(47) = 1.6$; $p = 0.11$
Caudate	$F_{1,39} = 0.80$; $p = 0.38$	$t(41) = 2.9$; $p = 0.099$	$t(41) = 0.23$; $p = 0.64$	$F_{1,47} = 0.42$; $p = 0.52$	$t(47) = 1.1$; $p = 0.29$	$t(47) = 1.7$; $p = 0.10$

	Clinical Tremor Score			Clinical Bradykinesia Score		
Seed Region	***β***	***t***	***p***	***β***	***t***	***p***
GPi	0.48	2.2	0.048[a]	0.29	1.1	0.30
GPe	0.55	2.6	0.022[a]	0.056	0.20	0.84
Putamen	0.78	5.2	<0.001[a]	0.24	0.90	0.39
Caudate	0.11	0.42	0.68	−0.12	−0.45	0.66

This table shows the inferential statistics concerning comparisons of striatopallidal functional connectivity between groups. Functional connectivity was defined as the coupling (β values) between each striatopallidal seed region (globus pallidus internus [GPi], globus pallidus externus [GPe], putamen, or caudate) and the portion of motor cortex showing tremor-related activity (see Fig 1). The amount of dopaminergic medication (liposome-encapsulated dichloromethylene diphosphonate) was added as a covariate of no interest to all analyses. First, we tested for differences in functional connectivity between the 2 Parkinson disease (PD) groups (factor Group: tremor-dominant vs nontremor PD) and the 2 hemispheres (factor Side: most-affected vs least-affected) (top left). Second, we tested for differences between healthy controls and left hemisphere-affected tremor-dominant patients (factor Group), and hemispheres (factor Side: left vs right hemisphere). Both analyses showed increased GPi/putamen connectivity with the motor cortex in the most-affected hemisphere of tremor-dominant PD. Third, we correlated the relative increase in striatopallidal connectivity with tremor severity (both expressed as the difference between most-affected and least-affected sides) (bottom left). This showed that GPi/GPe/putamen connectivity with the motor cortex was larger in patients with higher tremor scores. Fourth, we performed the same analysis for bradykinesia scores; this did not reveal significant effects (bottom right).
[a]Significant effects ($p < 0.05$).

interactions between the basal ganglia and the MC, as seen in tremor-dominant PD. Electrophysiological recordings in MPTP-treated vervet monkeys (that develop a parkinsonianlike resting tremor) support this suggestion. These monkeys show increased functional connectivity between the pallidum and MC,[28] presumably as a consequence of increased synchrony among pallidal neurons.[29] Depletion of dopamine, which is believed to separate the activity of different striatopallidal subcircuits, may underlie these changes.[29] Observations from postmortem studies in PD patients fit with this possibility, showing increased neuronal cell death in the retrorubral midbrain of tremor-dominant patients,[21] which sends dopaminergic projections to the pallidum[30] and to the subthalamic nucleus.[31] The increased coupling between GPi and MC could directly relay tremor-related oscillations from the basal ganglia toward the corticospinal tract.[32] However, this scenario would not explain why coherence between pallidal activity and resting tremor is only transient and inconsistent,[9,10] or why the cerebellar thalamus (VIM) is consistently and necessarily involved in resting tremor.[12,13] We suggest an alternative possibility that would accommodate these observations: transient increases in basal ganglia–MC coupling could trigger the generation of tremor-related oscillations within the VIM–MC–CBLM circuit. This scenario fits with the

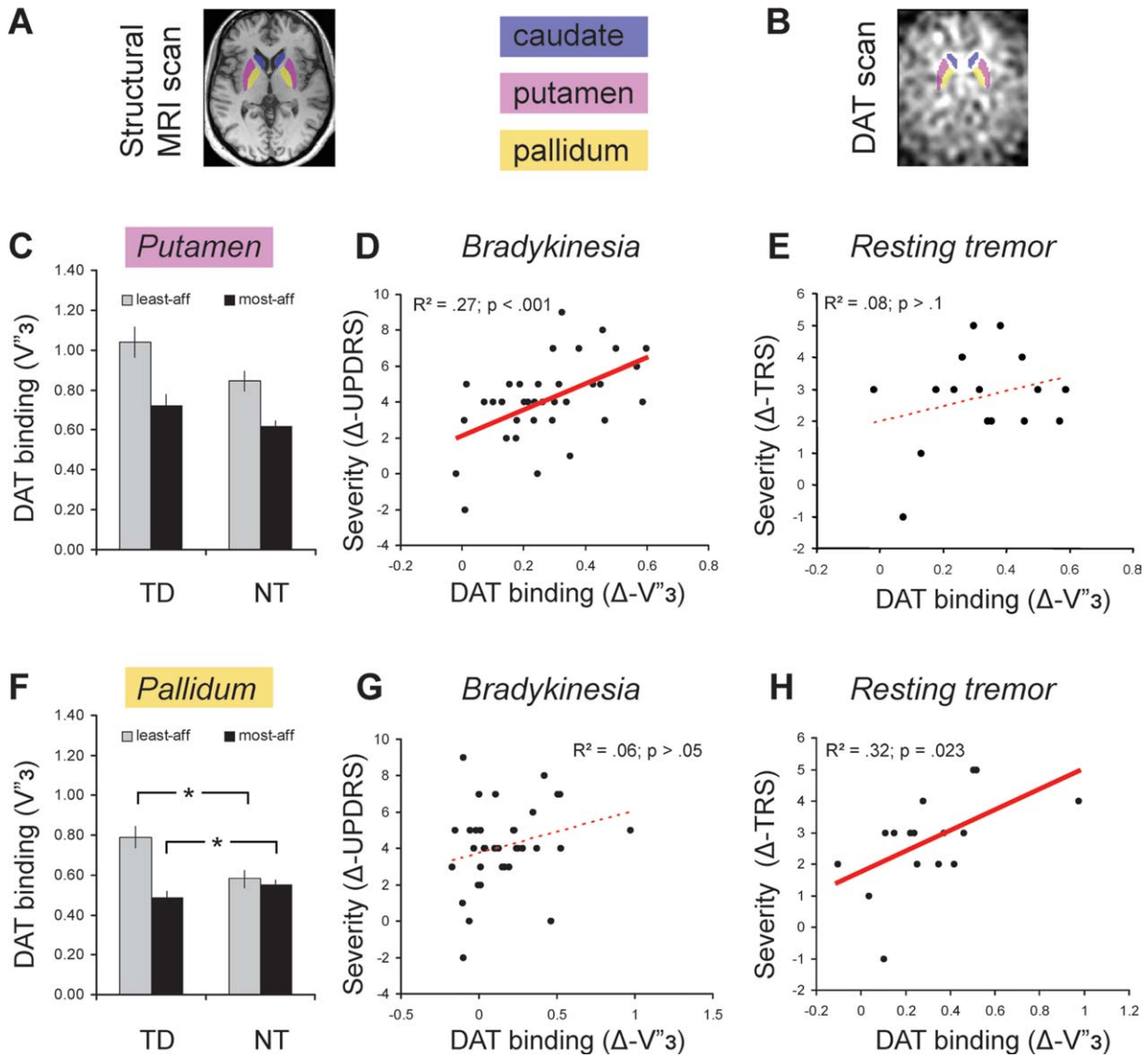

FIGURE 3: Imaging of the dopamine transporter (DAT). We quantified presynaptic DAT binding (using [I-123]FP-CIT single photon emission computed tomography [SPECT]) in the putamen (pink) and pallidum (orange), separately for tremor-dominant and nontremor Parkinson disease patients, and for the most-affected and least-affected hemisphere. (A) Pallidum, putamen, and caudate were defined based on each patient's structural magnetic resonance imaging (MRI) scan. (B) We overlaid these images onto each patient's SPECT scan and calculated the average DAT binding across each region, separately for each hemisphere. (C, F) Average DAT binding (on the y-axis, mean V″3 ± standard error of the mean) in the putamen (C) and pallidum (F). (D, G) Correlation between regional DAT binding (on the x-axis, difference between both sides, Δ-V″3) and bradykinesia severity (on the y-axis, difference between both sides, Δ-Unified Parkinson Disease Rating Scale [UPDRS]). (E, H) Correlation between regional DAT binding and resting tremor severity (on the y-axis, difference between both sides, Δ-Tremor Rating Scale [TRS]). For DAT binding in the caudate, see Supplementary Figure 4. aff = affected; TD = tremor-dominant PD; NT = non-tremor PD.

general notion that the thalamocortical system, with strong reciprocal anatomical connections[26] and nonlinear oscillatory dynamics,[7] is inherently unstable and particularly sensitive to modulatory influences.[33] More precisely, it is known that thalamic neurons can adopt 2 oscillatory modes, depending on their membrane potential[7]; a slight depolarization produces oscillations at 10Hz (in the range of physiological tremor[34]), whereas hyperpolarized cells (as found in the thalamus of tremor-dominant PD patients[35]) fire at 6Hz. However, because the thalamic recipient of pallidal output (nucleus ventralis oralis posterior) and the VIM nucleus are not directly connected,[18] interactions between the basal ganglia and cerebellar loops must take place at the cortical level.[16] These physiological and anatomical considerations, together with the present findings, suggest that pathological pallidal responses at the onset of tremor episodes hyperpolarize VIM neurons through the MC, triggering sustained periods of oscillations at tremor frequency within the VIM–MC–CBLM circuit.

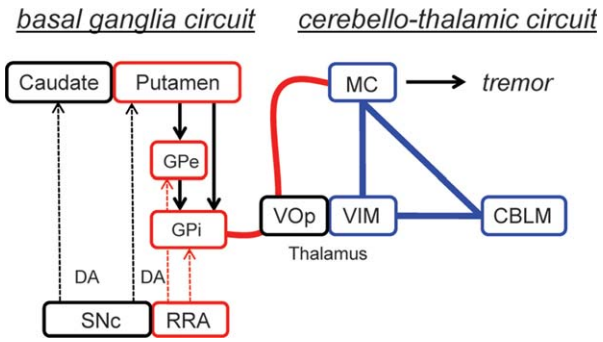

FIGURE 4: A model of cerebral mechanisms underlying Parkinson disease (PD) resting tremor. We propose that PD resting tremor emerges from the ventral intermediate nucleus of the thalamus (VIM)–motor cortex (MC)–cerebellum (CBLM) circuit (in blue), when triggered by transient pathological signals from the basal ganglia motor loop (in red). In tremor-dominant PD, the basal ganglia (globus pallidus internus [GPi], globus pallidus externus [GPe], and putamen) have increased connectivity with the VIM–MC–CBLM circuit through the MC (*thick red line*), and the basal ganglia are activated at critical time points in the tremor cycle (onset/offset of tremor episodes). These alterations may be caused by loss of dopaminergic projections from the retrorubral area of the midbrain (RRA; in red)[21] to the GPi and GPe.[30] These alterations are different from the dopaminergic denervation of the striatum, observed across different PD subtypes and associated with bradykinesia and rigidity. VOp = thalamic ventralis oralis posterior nucleus. DA = dopamine; SNc = substantia nigra pas compacta.

Interpretational Issues

Because activity in the basal ganglia increased at the onset of tremor episodes, we interpret this effect as representing a trigger for tremor-related responses within the cerebellothalamocortical circuit. This interpretation would fit with findings from deep brain surgery,[14,15] where interference with basal ganglia output can arrest tremor. However, fMRI is a correlational technique, and the effects we report may also be reactive rather than causative. To distinguish between these possibilities, future electrophysiological studies could test how activity in multiple nodes of the striatopallidal and corticocerebellar loops is temporally coordinated at transition points in tremor amplitude. Likewise, limited temporal resolution did not allow us to define the neural structures that determine the frequency at which PD resting tremor occurs. Because tremor cells are observed both in the basal ganglia[9,11] and in the cerebellothalamic circuit,[12] the basal ganglia may initiate oscillations at tremor frequency in the cerebellothalamic circuit, causing it to resonate at this frequency.

Because the pallidum contains relatively few DATs, it could be argued that the pallidal SPECT results are driven by spillover from the putamen. However, whereas this possibility predicts similar effects across pallidum and putamen, we observed opposite group effects in each area. Furthermore, clinical tremor severity was uniquely correlated with pallidal DAT binding, even when correcting for putaminal DAT. Finally, the SPECT signal in each striatopallidal region was at least 150% of that in the occipital cortex, a strong indication that it reflects DAT binding.[36]

Conclusions

This study shows that increased interactions between the basal ganglia and a distinct cerebellothalamic circuit mediate the occurrence of PD resting tremor. We propose that dopaminergic alterations in the pallidum trigger hyperactivity in the cerebellothalamic circuit, leading to resting tremor. These findings provide a possible solution to a longstanding mystery, that is, why a cerebellothalamic circuit is hyperactivated in PD, a disorder characterized by basal ganglia dysfunction. Furthermore, our findings may open the possibility to control resting tremor by transiently interfering with the basal ganglia triggering mechanism, rather than by complete ablation of basal ganglia or thalamic nodes of those circuits.

Acknowledgment

This work was supported by the Alkemade-Keuls Foundation (B.R.B.) and NWO (VIDI grant No. 016.076.352 to B.R.B.; VIDI grant No. 452-03-339 to I.T.). DAT was a kind gift of GE Healthcare, Eindhoven, the Netherlands.

We thank Dr J. Booij for helpful advice

R.C.H., I.T., and B.R.B. designed the study, interpreted the data, and wrote the paper. R.C.H. and B.R.B. recruited and assessed the patients. R.C.H. collected the fMRI data and conducted the analyses with help of I.T. M.J.R.J. and W.J.G.O. collected the SPECT data.

Potential Conflicts of Interest

Nothing to report.

References

1. Kish SJ, Shannak K, Hornykiewicz O. Uneven pattern of dopamine loss in the striatum of patients with idiopathic Parkinson's disease. Pathophysiologic and clinical implications. N Engl J Med 1988; 318:876–880.
2. Pirker W. Correlation of dopamine transporter imaging with parkinsonian motor handicap: how close is it? Mov Disord 2003; 18(suppl 7):S43–S51.
3. Fukuda M, Barnes A, Simon ES, et al. Thalamic stimulation for parkinsonian tremor: correlation between regional cerebral blood flow and physiological tremor characteristics. Neuroimage 2004; 21:608–615.
4. Timmermann L, Gross J, Dirks M, et al. The cerebral oscillatory network of parkinsonian resting tremor. Brain 2003;126: 199–212.

5. Gross J, Timmermann L, Kujala J, et al. The neural basis of intermittent motor control in humans. Proc Natl Acad Sci U S A 2002; 99:2299–2302.
6. Boecker H, Weindl A, Brooks DJ, et al. GABAergic dysfunction in essential tremor: an 11C-flumazenil PET study. J Nucl Med 2010; 51:1030–1035.
7. Llinas RR. The intrinsic electrophysiological properties of mammalian neurons: insights into central nervous system function. Science 1988;242:1654–1664.
8. Rodriguez-Oroz MC, Jahanshahi M, Krack P, et al. Initial clinical manifestations of Parkinson's disease: features and pathophysiological mechanisms. Lancet Neurol 2009;8:1128–1139.
9. Hurtado JM, Gray CM, Tamas LB, et al. Dynamics of tremor-related oscillations in the human globus pallidus: a single case study. Proc Natl Acad Sci U S A 1999;96:1674–1679.
10. Raz A, Vaadia E, Bergman H. Firing patterns and correlations of spontaneous discharge of pallidal neurons in the normal and the tremulous 1-methyl-4-phenyl-1,2,3,6-tetrahydropyridine vervet model of parkinsonism. J Neurosci 2000;20:8559–8571.
11. Levy R, Hutchison WD, Lozano AM, et al. High-frequency synchronization of neuronal activity in the subthalamic nucleus of parkinsonian patients with limb tremor. J Neurosci 2000;20: 7766–7775.
12. Lenz FA, Kwan HC, Martin RL, et al. Single unit analysis of the human ventral thalamic nuclear group. Tremor-related activity in functionally identified cells. Brain 1994;117(pt 3):531–543.
13. Benabid AL, Pollak P, Gervason C, et al. Long-term suppression of tremor by chronic stimulation of the ventral intermediate thalamic nucleus. Lancet 1991;337:403–406.
14. Krack P, Pollak P, Limousin P, et al. Stimulation of subthalamic nucleus alleviates tremor in Parkinson's disease. Lancet 1997;350: 1675.
15. Lozano AM, Lang AE, Galvez-Jimenez N, et al. Effect of GPi pallidotomy on motor function in Parkinson's disease. Lancet 1995; 346:1383–1387.
16. Deuschl G, Raethjen J, Baron R, et al. The pathophysiology of parkinsonian tremor: a review. J Neurol 2000;247(suppl 5):V33–V48.
17. Hoover JE, Strick PL. The organization of cerebellar and basal ganglia outputs to primary motor cortex as revealed by retrograde transneuronal transport of herpes simplex virus type 1. J Neurosci 1999;19:1446–1463.
18. Percheron G, Francois C, Talbi B, et al. The primate motor thalamus. Brain Res Brain Res Rev 1996;22:93–181.
19. Hoshi E, Tremblay L, Feger J, et al. The cerebellum communicates with the basal ganglia. Nat Neurosci 2005;8:1491–1493.
20. Bernheimer H, Birkmayer W, Hornykiewicz O, et al. Brain dopamine and the syndromes of Parkinson and Huntington. Clinical, morphological and neurochemical correlations. J Neurol Sci 1973; 20:415–455.
21. Hirsch EC, Mouatt A, Faucheux B, et al. Dopamine, tremor, and Parkinson's disease. Lancet 1992;340:125–126.
22. Jankovic J, McDermott M, Carter J, et al. Variable expression of Parkinson's disease: a base-line analysis of the DATATOP cohort. The Parkinson Study Group. Neurology 1990;40:1529–1534.
23. Langston JW, Widner H, Goetz CG, et al. Core assessment program for intracerebral transplantations (CAPIT). Mov Disord 1992; 7:2–13.
24. Helmich RC, Derikx LC, Bakker M, et al. Spatial remapping of cortico-striatal connectivity in Parkinson's disease. Cereb Cortex 2010;20:1175–1186.
25. Evrard HC, Craig AD. Retrograde analysis of the cerebellar projections to the posteroventral part of the ventral lateral thalamic nucleus in the macaque monkey. J Comp Neurol 2008;508: 286–314.
26. Kultas-Ilinsky K, Sivan-Loukianova E, Ilinsky IA. Reevaluation of the primary motor cortex connections with the thalamus in primates. J Comp Neurol 2003;457:133–158.
27. Vallbo AB, Wessberg J. Organization of motor output in slow finger movements in man. J Physiol 1993;469:673–691.
28. Rivlin-Etzion M, Marmor O, Saban G, et al. Low-pass filter properties of basal ganglia cortical muscle loops in the normal and MPTP primate model of parkinsonism. J Neurosci 2008;28: 633–649.
29. Bergman H, Feingold A, Nini A, et al. Physiological aspects of information processing in the basal ganglia of normal and parkinsonian primates. Trends Neurosci 1998;21:32–38.
30. Jan C, Francois C, Tande D, et al. Dopaminergic innervation of the pallidum in the normal state, in MPTP-treated monkeys and in parkinsonian patients. Eur J Neurosci 2000;12:4525–4535.
31. Francois C, Savy C, Jan C, et al. Dopaminergic innervation of the subthalamic nucleus in the normal state, in MPTP-treated monkeys, and in Parkinson's disease patients. J Comp Neurol 2000; 425:121–129.
32. McAuley JH, Marsden CD. Physiological and pathological tremors and rhythmic central motor control. Brain 2000;123(pt 8): 1545–1567.
33. Crick F, Koch C. Constraints on cortical and thalamic projections: the no-strong-loops hypothesis. Nature 1998;391:245–250.
34. Deuschl G, Raethjen J, Lindemann M, et al. The pathophysiology of tremor. Muscle Nerve 2001;24:716–735.
35. Magnin M, Morel A, Jeanmonod D. Single-unit analysis of the pallidum, thalamus and subthalamic nucleus in parkinsonian patients. Neuroscience 2000;96:549–564.
36. Laruelle M, Slifstein M, Huang Y. Relationships between radiotracer properties and image quality in molecular imaging of the brain with positron emission tomography. Mol Imaging Biol 2003; 5:363–375.
37. Dubois B, Slachevsky A, Litvan I, et al. The FAB: a Frontal Assessment Battery at bedside. Neurology 2000;55:1621–1626.
38. Stacy MA, Elble RJ, Ondo WG, et al. Assessment of interrater and intrarater reliability of the Fahn-Tolosa-Marin Tremor Rating Scale in essential tremor. Mov Disord 2007;22:833–838.
39. Atkinson JD, Collins DL, Bertrand G, et al. Optimal location of thalamotomy lesions for tremor associated with Parkinson disease: a probabilistic analysis based on postoperative magnetic resonance imaging and an integrated digital atlas. J Neurosurg 2002; 96:854–866.
40. Eickhoff SB, Stephan KE, Mohlberg H, et al. A new SPM toolbox for combining probabilistic cytoarchitectonic maps and functional imaging data. Neuroimage 2005;25:1325–1335.
41. Morel A, Magnin M, Jeanmonod D. Multiarchitectonic and stereotactic atlas of the human thalamus. J Comp Neurol 1997;387: 588–630.
42. Hirai T, Jones EG. A new parcellation of the human thalamus on the basis of histochemical staining. Brain Res Brain Res Rev 1989; 14:1–34.
43. Hassler R. Architectonic organization of the thalamic nuclei. In: Walker AE, ed. Stereotaxy of the Human Brain. Anatomical, Physiological and Clinical Applications. New York: Georg Thieme Verlag, 1982.